

Modulation of the aerosol absorption and single-scattering albedo in

P2.2 Southwest Asia due to large scale and sea breeze circulations.

Joanna Remiszewska
Institute of Geophysics, Polish Academy of Sciences, Poland

Krzysztof M. Markowicz
Institute of Geophysics, Warsaw University, Warsaw, Poland

Elizabeth A. Reid, Jeffrey S. Reid
Naval Research Laboratory, Marine Meteorology Division, Monterey, CA

Marcin L. Witek
Institute of Geophysics, Warsaw University, Warsaw, Poland

Abstract

Spectral aerosol particle absorption properties in the Arabian Gulf region were observed during the United Arab Emirates Unified Aerosol Experiment (UAE2) in August to September 2004. Measurements were taken at a coastal site located 60 km northeast of Abu Dhabi, the capital of the United Arab Emirates, allowing characterization of pollution and dust particle absorption properties in a highly heterogeneous environment. A large diurnal modulation was observed due to (a) strong sea- and land-breeze and (b) changes in prevailing large scale flow. During the night, stagnating air resulted in gradual accumulation of pollution with maximum absorption in the early morning hours. The rising sun increased both the depth of the boundary layer and the temperature of the

interior desert, resulting in strong and sudden sea-breeze onset, which ventilated the polluted air accumulated during the night. Our observations show that the onshore winds brought cleaner air resulting in decreasing values of the absorption coefficient and increasing values of the single-scattering albedo (ω_0). The mean value of the absorption coefficient at 550 nm measured during the sea breeze was 10.2 Mm⁻¹ while during the land breeze it was 13.8 Mm⁻¹. Large scale transport also strongly influenced particle fine/coarse partition with “northern” flow bringing pollution particles and “southern” flow bringing more dust.

1. INTRODUCTION.

The importance of aerosol light-absorption in the atmosphere’s radiative budget as well as in satellite retrievals is universally recognized. Despite this, a great a deal of disagreement occurs within the scientific community. For example, consider airborne dust. Optical properties of dust have been studied extensively using remote sensing

corresponding author address: Krzysztof M. Markowicz, Warsaw Univ., Inst. Of Geophysics, 02-093 Warsaw, Poland, email:kmark@igf.fuw.edu.pl

[Alpert and Ganor, 2001; Kalashnikova, et al., 2005; Reid, et al., 2003; Tanre, et al., 2003] and in situ measurements [Haywood, et al., 2001; Tanre, et al., 2003]. In general, there is considerable divergence between these methods, with reported single-scattering albedo values at 550 nm for dust ranging from 0.888 [Hess, et al., 1998] to 0.99 [Haywood, et al., 2003].

There are a number of reasons why such divergence occurs, including in situ absorption methodologies that have been repeatedly questioned [Bond and Bergstrom, 2006]. In order to reconcile these questions, a consistent set of measurements needs to be made in which the influence of physical parameters on the system can be studied along with response of the individual methods. For example, one would want to compare periods dominated by coarse mode particles with fine mode dominated conditions. Changing particle chemistries would also be beneficial, and humidity impacts need to be characterized. All of these conditions are met in Southwest Asia, where researchers can take advantage of varying regional aerosols driven by the physical meteorology.

The region surrounding the Arabian Gulf has recently been identified as the world's third largest dust source [Leon and Legrand, 2003], having maximum dust source activity during the spring and summer. The Arabian Gulf provides a unique laboratory to study the properties of dust and, as this region is a large source of anthropogenic emissions [Langner, et al., 1992], dust's interaction

with pollution can also be investigated. Atmospheric pollution is mostly through emission from local refineries, factories and fossil fuel combustion, though there is also significant transport from the Indian sub-continent. The concentration of aerosol particles depends on many factors including meteorological conditions [Leon and Legrand, 2003] and atmospheric circulation [Li and Ramanathan, 2002].

Despite the uniqueness of the region, the aerosol optical properties in the Arabian Gulf region are not well characterized. Previous ground and airborne measurements were made in the spring and summer of 1991 [Draxler, et al., 1994; Hobbs and Radke, 1992; Nakajima, et al., 1996] and were focused on the Kuwait oil fires. To our knowledge, the only published study of background conditions of aerosol optical properties in the region utilized direct sun and sky scanning radiometers [Smirnov, et al., 2002] and presented spectral dependency of the single scattering albedo (SSA) for dusty and non-dusty conditions.

Because the Arabian Gulf region's atmosphere is conducive to investigation of the fidelity of remote sensing systems, the United Arab Emirates (UAE) Unified Aerosol Experiment (UAE²) was performed. Conducted in August and September of 2004, UAE² included a comprehensive calibration and validation component to study the impact of dust absorption on space and surface based remote sensing retrievals over dark and bright surfaces. Two surface atmospheric research super-

sites and fifteen Aerosol Robotic Network Sun Photometers (AERONET) sites were deployed in coastal and desert regions of the UAE. One of the two surface stations, the Naval Research Laboratory's Mobile Atmospheric Aerosol and Radiation Characterization Observatory (MAARCO) was located on the Arabian Gulf coast approximately 60 km northeast of Abu Dhabi, away from the primary city plume. This location allowed studies of aerosol properties over coastal desert as modulated by the strong sea and land breeze circulations.

The purpose of this study is to extend previous knowledge and present the absorption coefficients and single scattering albedo measured in the coastal region of the Arabian Gulf [Draxler, et al., 1994; Hobbs and Radke, 1992; Nakajima, et al., 1996; Smirnov, et al., 2002]. This will provide baseline absorption data for many subsequent manuscripts that will examine aerosol particle properties and remote sensing algorithm fidelity. The results are based on the data collected during several weeks of measurements performed at the MAARCO facility.

2. INSTRUMENTS AND METHODS

In this section we describe instrumentation and methods for derivation of the absorption coefficient and the atmospheric single scattering albedo.

SCATTERING COEFFICIENT.

The aerosol scattering (σ_{scat}) and the hemispheric backscattering coefficients (σ_{bscat}) were measured by a TSI 3563 nephelometer at three wavelengths: 450,

550, and 700 nm. The instrument detects total scattered light between 7-170 degrees. Truncation and non-lambertian light source corrections were applied [Anderson, et al., 1996; Heintzenberg and Charlson, 1996]. During the experiment two nephelometers were simultaneously operated; one at near-atmospheric conditions and the other one at constant relative humidity of about 35 %.

Air was sampled from a total suspended particulate matter (TSP) inlet that fed the in-situ aerosol instruments. Consequently, the instruments measured fine and coarse mode simultaneously. To separate the contributions, often it is assumed that the scattering σ_{scat} is given by the following power law

$$\sigma_{\text{scat}} = \beta \lambda^{-\alpha}, \quad (1)$$

where Ångstrom coefficient α is given by:

$$\alpha_{\text{neph}} = \frac{-\log\left(\frac{\sigma_{\text{scat},450}}{\sigma_{\text{scat},700}}\right)}{\log\left(\frac{450}{700}\right)}, \quad (2)$$

and $\sigma_{\text{scat},450}$, $\sigma_{\text{scat},700}$ are scattering coefficients at 450 nm and 700 nm.

In general, α increases with the decreasing particle size and is smaller when large mode particles dominate the size distribution.

THE ABSORPTION COEFFICIENT.

The absorption coefficient was derived from Magee Scientific aethalometer (AE30) measurements. This instrument is designed for real-time continuous measurements of black carbon aerosol particle concentration [Hansen, et al., 1996]. The aethalometer continuously draws air samples through the inlet port, depositing the aerosols on a

fibrous filter media while performing continuous optical measurements of that filter media. Two detectors monitor the light transmission through the filter; one measures the light beam attenuation through the sample and filter and the other measures the light passing through a clean, reference filter section. The aethalometer measures the transmission through the filter over the wide spectrum of wavelengths, in our case 370, 430, 470, 520, 590, 700, 880 nm, and computes and reports the aerosol mass concentration [ng m^{-3}].

We use the two-stream approximation described by [Bohren, 1987] and [Arnott, et al., 2005]; an iterative method to match measured attenuation with attenuation predicted from the two-layer system in the two-stream approximation. In this method the only unknown quantity is the absorption coefficient.

From absorption and scattering coefficients we can compute the single scattering albedo

$$\omega_o \text{ defined as: } \omega_o = \frac{\sigma_{scat}}{\sigma_{scat} + \sigma_{abs}} \quad (3).$$

OTHER DATA

We used the HYSPLIT model [Draxler and Hess, 1998] to compute 72-hours backward trajectories for the MAARCO location (24.7°N, 54.7°E). The HYSPLIT (Hybrid Single-Particle Lagrangian Integrated Trajectory) model is a complete system for computing air parcel trajectories at different levels. We used HYSPLIT to compute trajectories at 10, 500, and 1000 meters above the ground to detect large-scale air

mass trajectories. The meteorological data is based on the NCEP Global Forecast System data with an assimilation system cycle of 6-hours and resolution 1x1 degree.

2. METEOROLOGICAL SUMMARY

THE DIURNAL CYCLE.

In this section we overview the daily land and sea breeze development. These intense local circulations are a regular phenomenon in the coastal region of the Arabian Gulf, in the absence of strong mesoscale flow [Zhu and Atkinson, 2004]. The onshore sea breeze develops about 13 local time (9 UTC) and lasts until 24 LT (18 UTC), and is associated with both an abrupt change of the wind direction and increased wind strength, in comparison to the land breeze. Winds associated with the sea breeze over the UAE coastline come mostly from the north with maximum velocities reaching values of about 6 ms^{-1} [Zhu and Atkinson, 2004], a value typical for a well developed moderate sea breeze [Miller, et al., 2003]. During the night, the land breeze is characterized by low wind speeds of about 3 ms^{-1} . Sea breeze is defined in terms of the wind direction; winds from 270 to 30 degrees define sea breeze, and winds from 30 to 270 degrees define land breeze. Figure 1 shows mean diurnal cycle of the wind direction (a), wind speed (b), relative humidity (c), and temperature (d). On these figures, dots indicate the sea breeze conditions. The data was collected from September 1 to September 22, 2004. Solid lines are 1-hour averages. Figure 1a

indicates that the diurnal change of wind direction is clockwise with fairly rapid sea breeze onset at around 9 UTC. One should be aware that these plots are averaged over approximately one month. In reality, values of meteorological fields are more abrupt than those presented in this section. It can be seen (Figure 1a) that on average the sea breeze duration is from 9 UTC to 18 UTC. The mean surface wind speed (Figure 1b) during land breeze remains in the range of $1\text{--}3\text{ ms}^{-1}$. From 3 UTC winds gradually increase until they reach the maximum of 6.0 ms^{-1} at 13 UTC and gradually decrease to 2.5 ms^{-1} at 19 UTC, after which they remain constant. It is evident that the largest values of wind speed are associated with the sea breeze cycle. Figure 1c and 1d present mean diurnal cycle of relative humidity (RH) and temperature, respectively. It is apparent that the diurnal cycle of RH is controlled by the solar insolation and corresponding surface temperature changes. The RH changes are inversely proportional to the mean surface temperature trend. The mean RH decreases gradually from 70 % to less than 50 % between 1–6 UTC. After the sea breeze onset RH increases gradually to 70% at the end of the day. Mean temperature varies from 30°C to 34°C . It reaches maximum value at 8 UTC (12 LT). The diurnal cycle of absolute humidity is presented in Figure 1e. The rapid increase starts in the morning at 6 UTC ending with the maximum value of about 21 g kg^{-1} at 18 UTC. This corresponds to both increased

surface temperature and flow onset from the Arabian Gulf. Beginning 8 UTC this trend reverses. Thus, it is observed that increased specific humidity correlates well with the duration of the sea breeze. The mean meteorological conditions of temperature and wind speed do not change considerably from the pattern described above.

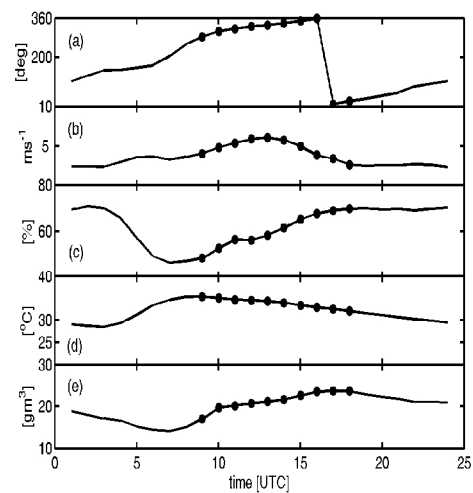


Figure 1. Mean diurnal cycle of: (a) wind direction, (b) wind speed, (c) relative humidity, (d) temperature, and (e) absolute humidity. Solid circles indicate sea breeze.

3. RESULTS.

3.1. DIURNAL CYCLE OF THE AEROSOL OPTICAL PROPERTIES.

In this section we present daily changes of the aerosol optical properties in relation to land and sea breeze onset.

The time series of absorption coefficients and atmospheric single scattering albedo are presented in Figure 2. The data were collected over the period of time from

August 27 to September 30, 2004 and averaged in one-hour bins. Characteristic regular minima in absorption coefficient values and respectively maxima in SSA are

apparent. The diurnal variability of these quantities is discussed later. In order to examine the wavelength dependence of SSA we introduce the Ångstrom-like coefficient defined for the single scattering albedo at 450 nm and 700nm. It is given by:

$$\alpha_{\omega} = \frac{-\log\left(\frac{\omega_{450}}{\omega_{700}}\right)}{\log\left(\frac{450}{700}\right)}, \quad (4)$$

where ω_{450} , ω_{700} denote single scattering albedo at 450 nm and 700 nm.

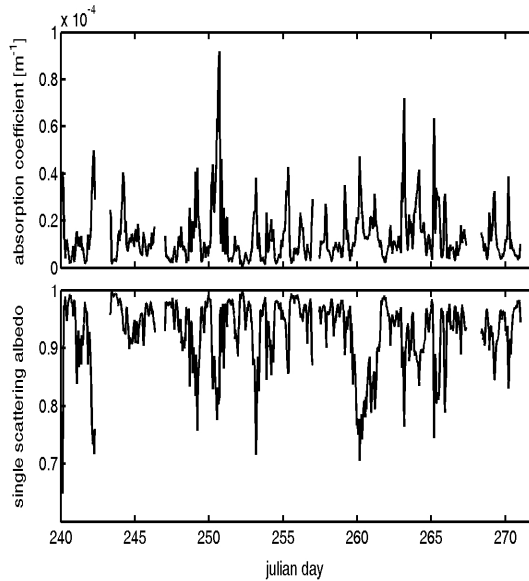


Figure 2. Time series of the absorption coefficient and single scattering albedo at 550 nm from August 27 to September 30, 2004. The data were averaged in 1 hour bins.

If α_{ω} is less than 0 it indicates that SSA increases with wavelength, while if α_{ω} is larger than 0, SSA decreases with wavelength. Figure 3 presents time-series of α_{ω} from August 27 to September 30, 2004. Clearly, wavelength dependency changes during the measurement time. We observe a few episodes when ω decreases with the wavelength as well as a few episodes when ω increases with the wavelength.

The mean diurnal cycles of the absorption coefficient and single scattering albedo are presented in Figure 4. These data were averaged over the period from August 27, 2004 to September 30, 2004 in one hour bins. The absorption coefficient is at maximum in the early morning at around 4 UTC because of weak winds and stable conditions. The absorption coefficient gradually decreases from about $2.4 \times 10^{-5} \text{ [m}^{-1}\text{]}$ at 550 nm to about $0.7 \times 10^{-5} \text{ [m}^{-1}\text{]}$, reaching minimum values between 10 UTC and 20 UTC. This is associated with the sea-breeze development and its ventilating effect. From about 18 UTC there is a gradual absorption increase which is related to wind shift and transport of pollution from land.

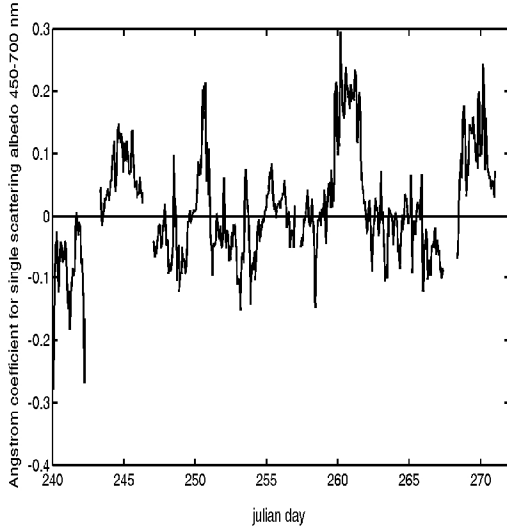


Figure 3. Ångström coefficient for single scattering albedo averaged in one-hour bins.

The behavior of the atmospheric single scattering albedo is strongly dependent on absorption coefficient. The developing sea-breeze results in an increase of SSA values between 9 UTC and 18 UTC, reaching a maximum of about 0.95 for the 550nm channel at 18 UTC; the time at which the absorption coefficient reaches minimum. The minimum value of the SSA, 0.88 at 550nm, occurs at 4 UTC and corresponds to the maximum value of the absorption coefficient. Table 1 presents mean values of the absorption coefficient and the atmospheric single scattering albedo during the sea- and land-breeze, and mean values of these quantities averaged over the period from August 27, 2004 to September 30, 2004.

Mean values of the atmospheric single-scattering albedo are similar in all channels, but closer examination of its spectral

dependence leads to the conclusion that it changes during the day. Between 13 UTC and 22 UTC the atmospheric SSA in the red wavelength is smaller than in the blue wavelength but this trend reverses as time progresses, suggesting a change in aerosol composition over the course of the day.

3.2. SYNOPTIC SCALE FLOW AND LOCAL SEA BREEZE EFFECTS.

Previous analysis focused on the local circulation and its influence on the aerosol optical properties. We will now discuss large-scale circulation impact on aerosol optical properties. As was discussed in the “Meteorological Summary” section we can distinguish three large-scale regimes in the region: (a) flow from the north (33% of all cases), (b) south (47%), and (c) “mixed” flow.

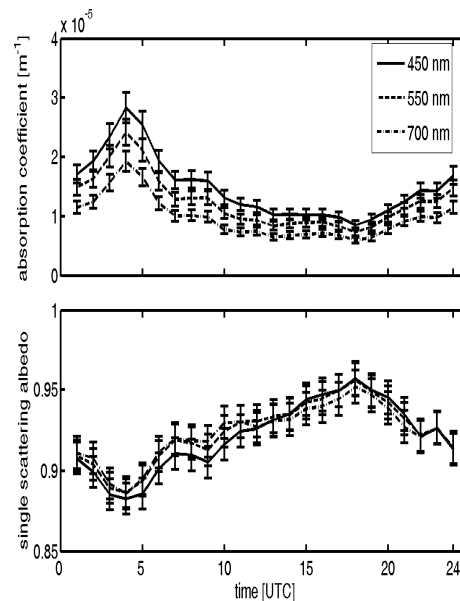


Figure 4. Diurnal cycle of the absorption coefficient and atmospheric single scattering albedo at three wavelengths:

450 nm, 550 nm, and 700 nm. The data was collected and averaged over the period of time from August 27 to September 30, 2004.

Figure 5 presents mean diurnal cycle of the Ångstrom exponent ($\alpha_{450-700nm}$) for each type of flow. It is apparent that the aerosol origin is an important factor determining the size of particles. The northern flow carries more fine particles – Ångstrom exponent exceeds unity with a mean value of 1.45. The southern flow is dominated by larger particles with mean value of Ångstrom exponent of 0.68.

Figure 6 presents mean diurnal cycles of absorption coefficient and SSA at 450, 550, 700 nm for three large-scale cases. Table 2 summarizes the mean values of absorption coefficient for northern, southern, and “mixed” flows.

It is apparent that northern flow carries more absorptive aerosol than the southern one. Also, the atmospheric single scattering albedo is greater for southern flow than for northern, with the difference increasing as the sea breeze develops. The atmospheric single-scattering albedo decreases with wavelength for aerosols transported from the north and increases when aerosols

come from the south (dust).

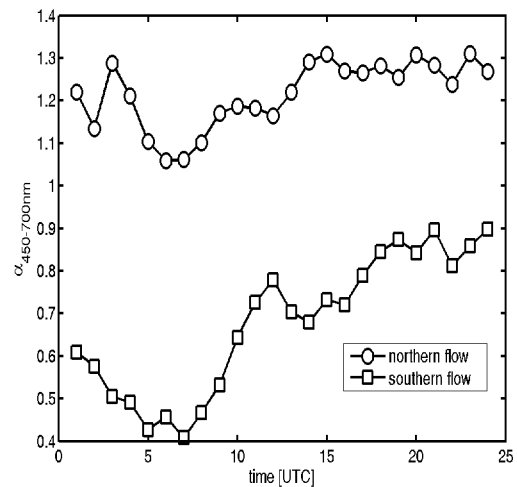


Figure 5. Mean diurnal cycle of the Ångstrom coefficient based on 450 and 700 nm nephelometer channels for northern and southern.

Table 3 provides information about the influence of the sea-land breeze circulation on the value of the absorption coefficient.

Mean values of absorption coefficients during the sea breeze are about 2 times less for the southern flow than for the northern. This is related to the influence of smaller anthropogenic aerosol particles coming from oil processing and industrial areas to the north; while the southern flow brings air with less anthropogenic pollution, but with more dust particles from the deserts in UAE, Oman and Saudi Arabia. The wavelength dependency of the atmospheric SSA for the northern flow presented in Figure 6 is characteristic of industrial aerosol [Dubovik, et al., 2002]. It is also consistent with the larger values of the absorption coefficient in comparison to the values observed for the southern flow.

It is clear from Figure 6 that of the rate of increase in the atmospheric SSA values during the sea breeze is more rapid for the southern flow. This is because the prevailing cleaner southern flow is interacting with the onshore winds. Sea breeze lasts from 9 UTC to 17 UTC; during which time we observe an increasing trend of the atmospheric SSA values from 0.91 at 550 nm to about 0.96 during the well-developed sea breeze. On the other hand, when air moves from the north carrying in industrial pollution, we observe only a slight increase in the atmospheric SSA values from 4 UTC to 19 UTC.

4. SUMMARY.

In the summer of 2004 the coastal region of the Arabian Gulf northeast of Abu Dhabi, the capital of the United Arab Emirates, was influenced by large-scale circulation, modulated by very intense land- and sea breeze circulation. The atmospheric aerosol single-scattering properties were strongly influenced by the synoptic scale and local scale systems. During the night, the stagnating air resulted in gradual accumulation of pollution with maximum absorption in the early morning hours. The rising sun increased the depth of the boundary layer and temperature of the interior desert, resulting in strong and sudden sea-breeze onset that ventilated polluted air accumulated during the night. However, the air over the Arabian Gulf and its surroundings is itself polluted, which we document on the basis of absorption and scattering measurements. In particular, the

synoptic “northern” flow brings smaller particles and the “southern” flow brings air with larger particles from dusty regions. This conceptual model is presented in Figure 14.

Mean value of the absorption coefficient at 550 nm during the land breeze is 35 % higher than during the sea breeze case. The atmospheric single-scattering albedo increases during the sea breeze reaching a maximum value of about 0.95 in the 550nm channel at 19 UTC. The 72-hour back trajectories computed using the HYSPLIT model provide means to identify the source region. We distinguish two main large-scale flows corresponding to 80 % of all cases. The “north flow” carries smaller particles with Ångstrom coefficient greater than 1 and mean value of 1.45.

Flow from south brings larger particles with mean value of the Ångstrom exponent of 0.68. Aerosols for the “north flow” case are more absorptive than aerosol for the “south flow” case. Mean value of the absorption coefficient at 550 nm for the northern flow is 14.89 Mm^{-1} and for the southern flow is 10.85 Mm^{-1} . Sea-breeze influence on the optical properties of aerosols is greater in the case of the “south flow”. Mean values of the absorption coefficient at 550 nm during the sea breeze for the southern flow are almost 2 times less than for northern cases.

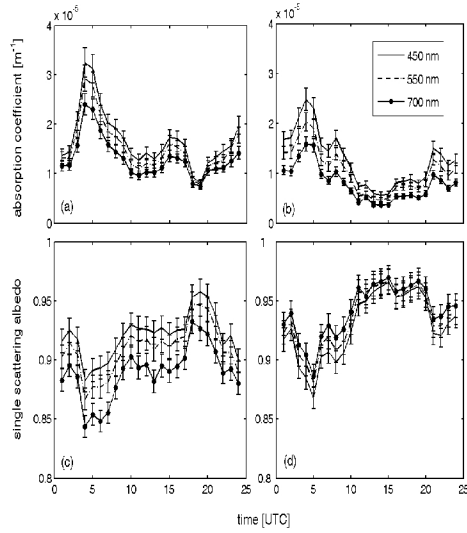


Figure 6. Mean diurnal cycle of the absorption coefficient at 450 nm, 550 nm, and 700 nm for northern flow (a) and southern flow (b) and mean diurnal cycle of the atmospheric single scattering albedo for northern (c) and southern flow (d).

Wavelength [nm]	$\sigma_{\text{abs,mean}} [\text{Mm}^{-1}]$	$\sigma_{\text{abs,sea breeze}} [\text{Mm}^{-1}]$	$\sigma_{\text{abs,land breeze}} [\text{Mm}^{-1}]$	ω_{mean}	$\omega_{\text{sea breeze}}$	$\omega_{\text{land breeze}}$
450	15 ± 1.4	11.2 ± 1.0	17.4 ± 1.6	0.92 ± 0.01	0.93 ± 0.01	0.91 ± 0.01
550	12 ± 1.1	10.2 ± 0.92	13.8 ± 1.24			
700	10 ± 0.9	7.3 ± 0.66	11.6 ± 1.04			

Table 1. Mean values of the absorption coefficient at 450, 550, 700 nm averaged over the period from August, 27 to September, 30 of 2004 ($\sigma_{\text{abs,mean}}$) for the sea breeze $\sigma_{\text{abs,sea breeze}}$ and for the land-breeze $\sigma_{\text{abs,land breeze}}$. Also presented are the SSA values.

Wavelength [nm]	σ_{abs} [Mm ⁻¹]		
	Northern flow	Southern flow	“Mixed” flow
450	16.36 ± 1.47	12.15 ± 1.09	16.49 ± 1.48
550	14.89 ± 1.34	10.05 ± 0.90	14.14 ± 1.27
700	12.73 ± 1.14	7.61 ± 0.68	10.67 ± 0.96

Table 2. Mean values of the absorption coefficient (σ_{abs}) at 450, 550, and 700 nm for northern, southern and “mixed” flows.

Wavelength [nm]	$\sigma_{\text{abs,sea breeze}}$ [Mm ⁻¹]		$\sigma_{\text{abs,land breeze}}$ [Mm ⁻¹]	
	Northern flow	Southern flow	Northern flow	Southern flow
450	14.52 ± 1.31	9.14 ± 0.82	19.15 ± 1.72	14.18 ± 1.28
550	13.23 ± 1.19	7.65 ± 0.69	17.4 ± 1.57	11.67 ± 1.05
700	11.37 ± 1.02	5.94 ± 0.55	14.79 ± 1.33	8.74 ± 0.79

Table 3. Mean values of absorption coefficient during sea breeze ($\sigma_{\text{abs,sea breeze}}$) and land breeze ($\sigma_{\text{abs,land breeze}}$) for northern, southern flow.

Acknowledgments

We (JR and KM) would like to acknowledge support from ONR Global. ONR Code 32 and NASA ESE Radiation Sciences Program provided NRL’s participation in this effort.

Conference presentation was supported by EVK2-CT2002-80010-CESSAR EC V Framework Program project.

References

Alpert, P., and E. Ganor, Sahara mineral dust measurements from TOMS: Comparison to surface observations over the Middle East for the extreme dust storm, March 14-17, 1998, *Journal of Geophysical Research-Atmospheres*, 106, 18275-18286, 2001.

Anderson, T. L., D. S. Covert, S. F. Marshall, M. L. Laucks, R. J. Charlson, A. P. Waggoner, J. A. Ogren, R. Caldwell, R. L. Holm, F. R. Quant, G. J. Sem, A. Wiedensohler, N. A. Ahlquist, and T. S. Bates, Performance characteristics of a high-sensitivity, three-wavelength, total scatter/backscatter nephelometer, *Journal Of Atmospheric And Oceanic Technology*, 13, 967-986, 1996.

Arnott, W. P., K. Hamasha, H. Moosmuller, P. J. Sheridan, and J. A. Ogren, Towards aerosol light-absorption measurements with a 7-wavelength Aethalometer: Evaluation with a photoacoustic instrument and 3-wavelength nephelometer, *Aerosol Science And Technology*, 39, 17-29, 2005.

Bohren, C. F., Multiple scattering of light and some of its observable consequences, *American Journal of Physics*, 55, 524-533, 1987.

- Draxler, R. R., and D. G. Hess, An overview of the Hysplit_4 modeling system for trajectories, dispersion, and deposition, *Australian Meteorology Magazine*, 47, 295-308, 1998.
- Draxler, R. R., J. T. McQueen, and B. J. B. Stunder, An Evaluation of Air Pollutant Exposures Due to the 1991 Kuwait Oil Fires Using a Lagrangian Model, *Atmospheric Environment*, 28, 2197-2210, 1994.
- Hansen, A. D. A., H. Rosen, and T. Novakov, The Aethalometer - an Instrument for the Real-Time Measurement of Optical-Absorption by Aerosol-Particles, *Science of the Total Environment*, 36, 191-196, 1996.
- Haywood, J., P. Francis, S. Osborne, M. Glew, N. Loeb, E. Highwood, D. Tanre, G. Myhre, P. Formenti, and E. Hirst, Radiative properties and direct radiative effect of Saharan dust measured by the C-130 aircraft during SHADE: 1. Solar spectrum, *Journal Of Geophysical Research-Atmospheres*, 108, 2003.
- Haywood, J. M., P. N. Francis, M. D. Glew, and J. P. Taylor, Optical properties and direct radiative effect of Saharan dust: A case study of two Saharan dust outbreaks using aircraft data, *Journal of Geophysical Research-Atmospheres*, 106, 18417-18430, 2001.
- Heintzenberg, J., and R. J. Charlson, Design and applications of the integrating nephelometer: A review, *Journal Of Atmospheric And Oceanic Technology*, 13, 987-1000, 1996.
- Hess, M., P. Koepke, and I. Schult, Optical properties of aerosols and clouds: The software package OPAC, *Bulletin of the American Meteorological Society*, 79, 831-844, 1998.
- Hobbs, P. V., and L. F. Radke, Airborne Studies Of The Smoke From The Kuwait Oil Fires, *Science*, 256, 987-991, 1992.
- Kalashnikova, O. V., R. Kahn, I. N. Sokolik, and W. H. Li, Ability of multiangle remote sensing observations to identify and distinguish mineral dust types: Optical models and retrievals of optically thick plumes, *Journal of Geophysical Research-Atmospheres*, 110, 2005.
- Langner, J., H. Rodhe, P. J. Crutzen, and P. Zimmerman, Anthropogenic influence on the distribution of tropospheric sulphate aerosol, *Nature* 359, 712-716, 1992.
- Leon, J. F., and M. Legrand, Mineral dust sources in the surroundings of the north Indian Ocean, *Geophysical Research Letters*, 30, 2003.
- Li, F., and V. Ramanathan, Winter to summer monsoon variation of aerosol optical depth over the tropical Indian Ocean, *Journal of Geophysical Research-Atmospheres*, 107, 2002.
- Miller, S. T. K., B. D. Keim, R. W. Talbot, and H. Mao, Sea breeze: Structure, forecasting, and impacts, *Reviews of Geophysics*, 41, 2003.
- Nakajima, T., T. Hayasaka, A. Higurashi, G. Hashida, N. MoharramNejad, Y. Najafi, and H. Valavi, Aerosol optical properties in the Iranian region obtained by ground-based solar radiation measurements in the summer of 1991, *Journal Of Applied Meteorology*, 35, 1265-1278, 1996.
- Reid, J. S., J. E. Kinney, D. L. Westphal, B. N. Holben, E. J. Welton, S. C. Tsay, D. P. Eleuterio, J. R. Campbell, S. A. Christopher, P. R. Colarco, H. H. Jonsson, J. M. Livingston, H. B. Maring, M. L. Meier, P. Pilewskie, J. M. Prospero, E. A. Reid, L. A. Remer, P. B. Russell, D. L. Savoie, A. Smirnov, and D. Tanre, Analysis of measurements of Saharan dust by airborne and ground-based remote sensing methods during the Puerto Rico Dust Experiment (PRIDE), *Journal of Geophysical Research-Atmospheres*, 108, 2003.
- Smirnov, A., B. N. Holben, O. Dubovik, N. T. O'Neill, T. F. Eck, D. L. Westphal, A. K. Goroch, C. Pietras, and I. Slutsker, Atmospheric aerosol optical properties in the Persian Gulf, *Journal Of The Atmospheric Sciences*, 59, 620-634, 2002.
- Tanre, D., J. Haywood, J. Pelon, J. F. Leon, B. Chatenet, P. Formenti, P. Zhu, M., and B. W. Atkinson, Observed and modelled climatology of the land-sea breeze

circulation over the Persian Gulf,
International Journal Of Climatology, 24,
883-905, 2004.